

High-speed channel demixing by scanning interferometric focusing with binary transmission matrix

Xiaodong Tao^{*a}, Dare Bodington^b, Marc Reinig^a and Joel Kubby^a

^aW.M. Keck Center for Adaptive Optical Microscopy, Jack Baskin School of Engineering, University of California, Santa Cruz, CA 95064, USA; ^bThe Institute of Optics, University of Rochester, Rochester, New York 14627, USA

ABSTRACT

In this paper, we demonstrate a fast binary intensity modulation based on the measurement of the binary TM. For each correction, the binary TM was calculated based on measurements of the intensity change at the target with a series of input masks. After preloading the measurement masks, the DMD can run at full speed during measurement. The system allows dynamic focusing at 12.5 Hz with 1024 input modes, and more than 60 times intensity enhancement. We demonstrate focusing light through a highly dynamic scattering sample, a live drosophila embryo.

Keywords: Times Roman, image area, acronyms, references

1. INTRODUCTION

As light propagates through biological tissues, it can be refracted, scattered and absorbed, limiting the imaging resolution and depth. To correct the refractive aberration, adaptive optics (AO) has been extensively investigated for applications in optical microscopy [1]. As the imaging depth increases, AO becomes less effective for focusing light in the sample. Multiple scattering becomes a dominant factor limiting the image depth. However the amplitude of elastic scattering loss is noted to be an order of magnitude or more than that of absorption. Overcoming the elastic scattering can dramatically extend the light penetration depth. Thanks to the deterministic process of scattering, there exists a linear relationship between the input modes and the output modes of the wavefront, which can be described by a transmission matrix (TM) [2, 3]. To generate the desired optical field through scattering media, TM can be measured by using a LC-SLM and a full-field interferometric measurement. Then the light transmission can be completely controlled and the scattering media can act as a lens to transfer the image [4, 5]. To focus the beam through scattering tissue at a single or multiple output channels, iterative optimization methods have been demonstrated [6-8]. To obtain optimized focusing, thousands of degrees of freedom of the incident wavefront need to be modulated and measured. Recently another high speed light modulator, the digital micromirror device (DMD), has been used to compensate scattering in biological tissue [9-13]. It contains millions of fast switchable micromirrors to modulate the intensity of the light based on its two states. A commercially available DMD has frame rates up to 22 kHz and could have more than one million of pixels. The first demonstration of binary intensity modulation using a DMD was made by Mosk's group, where a sequential iterative algorithm was used to focus light through turbid media [9]. The lower efficiency of intensity modulation compared with phase modulation can be compensated by the large number of available channels on the DMD. Phase modulation on a DMD using a hologram was also proposed at the expense of phase resolution loss [10-11]. The resolution can be further improved by a superpixel-based spatial amplitude and phase modulation [12]. A genetic algorithm has also been used in binary intensity modulation to improve the performance of the optimization process [13].

In this paper, we demonstrate a fast binary intensity modulation based on the measurement of the binary TM. For each correction, the binary TM was calculated based on measurements of the intensity change at the target with a series of input masks. After preloading the measurement masks, the DMD can run at full speed during measurement. Compared with the optimization method, no feedback information is needed during the measurement. The proposed method only requires one measurement for each input mode. The total time for a single correction is only 75ms for 1024 input modes. The direct intensity modulation used in this paper has much higher light efficiency (60%) [10,11]. This is more suitable for applications that are sensitive to optical power loss. We demonstrate focusing light through a highly dynamic scattering sample, a live drosophila embryo.

2. MATERIALS AND METHODS

2.1 Measurement of the binary TM

Light transport through scattering medium can be characterized by a TM, which connects electric fields from the incoming and outgoing channels [2]. To focus the light through scattering medium at one output channel, the electric field at the output channel, E_{out} , can be considered as the sum of the contributions from all the input channels, which is given by,

$$E_{out} = KE = \sum_n k_n e_{in}^n \quad (1)$$

E is the input electric field vector, where e_{in}^n is the electric field at the nth input channel. K is the TM for a single output channel, where k_n connects the nth input channel and the output channel. When using a binary amplitude modulator, the goal is to open the input channels which can generate constructive interference at the target and block the other channels. The only information required is the binary state of each element in the transmission matrix, i.e. whether their relative phases are in the range of π .

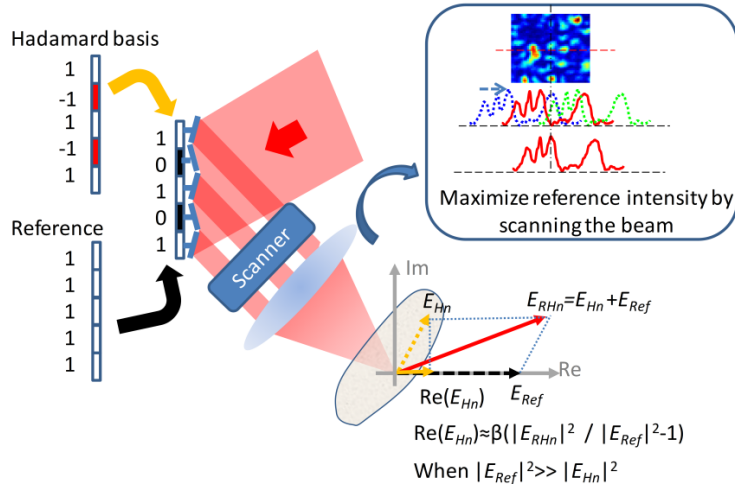


Figure 1. Principle of binary intensity modulation. The combination of the reference and Hadamard basis is displayed on the DMD. The amplitude at the output, $|E_{RHn}|^2$, can be used to calculate the binary TM. Higher reference intensity gives a more accurate measurement. By scanning the speckles around the target, the maximum reference intensity is achieved at the target before measurement of the binary TM.

When a plane wave e_0 reflects from a binary amplitude modulator, such as the DMD, the electric field after the modulator E_B , can be written as

$$E_B = Ae_0 \quad (2)$$

where $A = [a_1 \dots a_N]^T$ is the binary modulation vector. The electric field at the output can be written as

$$E_{out} = KE_B = KAe_0 \quad (3)$$

We first define a reference electric field at the output channel, when all channels are turned on,

$$E_{Ref} = KA_{Ref}e_0, \text{ where } A_{Ref} = [1 \dots 1]^T \quad (4)$$

Then to achieve constructive interference at the output, we need to block the channels which have destructive interference with E_{Ref} . That is to open the channels with output phase in the range of $(\varphi_{Ref} - \pi/2, \varphi_{Ref} + \pi/2)$ and block the

other channels as shown in Fig. 1(b), where φ_{Ref} is the phase of the reference. The resulting electric field at the output then becomes

$$E_{\text{out}} = KA_k e_0 \quad (5)$$

Since the input electric field e_0 is a plane wave, the binary modulation vector A_k is also a binary TM which contains binary information of the TM based on its relative phase to the reference electric field. For simplicity, we align the reference phasor E_{Ref} along the real axis. Therefore the elements of A_k , can be calculated as

$$a_n = \begin{cases} 1 & \text{Re}(k_n e_0) \geq 0 \\ 0 & \text{Re}(k_n e_0) < 0 \end{cases} \quad (6)$$

where $\text{Re}()$ is the real part of a complex vector. To obtain $\text{Re}(k_n e_0)$, we chose the Hadamard basis as the input basis because of its orthogonal property. The output electric field for different Hadamard modes is given by

$$[E_{H1} \ \cdots \ E_{HN}] = K[H_1 \ \cdots \ H_N]e_0 \quad (7)$$

where E_{Hn} is the output electric field for the nth Hadamard mode. H_n is the nth Hadamard mode defined as a $N \times 1$ vector, where N is the number of channels. Therefore $\text{Re}(Ke_0)$ can be calculated by

$$\text{Re}(Ke_0) = \frac{1}{N} [\text{Re}(E_{H1}) \ \cdots \ \text{Re}(E_{HN})] [H_1 \ \cdots \ H_N]^T \quad (8)$$

where $[\]^T$ is the transpose of the matrix. Although it is hard to directly measure $\text{Re}(E_{Hn})$, it can be estimated by the intensity of the sum of E_{Hn} and E_{Ref} at the output channel. Because values of the elements in the Hadamard matrix H_n are either -1 or 1, the addition of A_{ref} and a Hadamard mode can be obtained after the DMD,

$$E_{BI} = \frac{1}{2} (A_{\text{Ref}} + H_n) e_0 \quad (9)$$

where the elements of $\frac{1}{2} (A_{\text{Ref}} + H_n)$ are either 0 or 1, which can be perfectly modulated on the DMD. The output electric field is the summation of the reference electric field E_{Ref} and the electric field for a Hadamard mode E_{Hn} at the output channel as shown in Fig.1.

$$E_{RHn} = E_{Hn} + E_{\text{Ref}} \quad (10)$$

Then the relationship between $\text{Re}(E_{Hn})$ and $|E_{RHn}|$ can be calculated accordingly as

$$\text{Re}(E_{Hn}) \cong \beta \left(\frac{|E_{RHn}|^2}{|E_{\text{Ref}}|^2} - 1 \right) \quad (11)$$

If $|E_{\text{Ref}}|^2$ is sufficiently larger than $|E_{Hn}|^2$. From Eq. (8) and Eq. (11), a vector J based on the intensity measurement is obtained, which can be used to determine the final binary TM, A_k .

$$J = \left[|E_{RH1}|^2 \ \cdots \ |E_{RHN}|^2 \right] [H_1 \ \cdots \ H_N]^T \cong \gamma \text{Re}(Ke_0) \quad (12)$$

where $\gamma = \frac{N|E_{\text{Ref}}|^2}{\beta}$ is a constant and N is the number of the channels. Since half of the channels are turned on, the threshold T can be selected so that the sum of matrix elements A_k is equal to $N/2$. The final result can be calculated as

$$a_n = \begin{cases} 1 & j_n \geq T \\ 0 & j_n < T. \end{cases} \quad (13)$$

This calculation is based on the assumption that the intensity of E_{Ref} is sufficiently large. However the relatively low intensity of the reference field in the real situation introduces errors to Eqs. (11). To overcome this issue, a reference optimization process is performed by using a scanner in the system to steer the beam along one axis on the sample when all the micromirrors on the DMD are on as shown in Fig. 1. To evaluate the effect of the reference intensity on the performance of the binary intensity modulation, a Monte Carlo simulation was carried out by assuming a circular complex Gaussian distribution for the output electric field of each Hadamard mode.

With 10 samples on the scanning line, the error of the final pattern would be around 12.6%. Increasing the samples during scanning can further decrease the error. With 50 samples, the error can decrease to 10%. By applying this method, we can dramatically improve focusing through a scattering sample. Here the pattern shift could be caused by the memory effect. If the speckle patterns are totally uncorrelated after mirror scanning, the intensity of the speckles still obeys the negative exponential statistics. The above analysis is still valid. In applications for laser scanning imaging systems, the existing galvanometric mirrors in the system can be utilized for reference optimization, which can reduce the cost and complexity of the system.

2.2 System setup

The experimental setup is shown in Fig. 2. A DMD (DLi4130, 0.7" XGA, Digital Light Innovations) with 1024x768 mirrors and 22.727 kHz frames per second was used as a binary intensity modulator. A HeNe laser at 633nm (25-LHP-991, CVI Melles Griot) was employed as a light source in the experiment. In order to make the intensity more uniform across the aperture of the DMD, a telescope composed of lenses L1 (20x/0.40, Newport) and L2 ($f=150\text{mm}$, AC254-150-A, Thorlabs) expands the beam by 16.7 times. The output beam from the telescope with a $1/e^2$ diameter of 10.8 mm covers the exit pupil of the DMD. An iris diaphragm I1 was mounted after the telescope for avoiding artifacts from the edge of the window aperture coating on the DMD. The incident angle of the beam on the DMD was adjusted carefully to achieve the blaze condition when the reflected beam from the micro mirror lines up with the sixth order of the diffraction grating from the DMD. The majority of the energy is directed into the blazed order. The other orders were blocked by the iris diaphragm I2. The efficiency of the DMD, defined as the ratio of the reflected light to the incident light on the DMD, is around 60% when all mirrors are in the full on-state. The DMD is conjugated with the galvanometer by lenses L3 ($f=150\text{mm}$, AC254-150-A, Thorlabs) and L4 ($f=50\text{mm}$, AC254-50-A, Thorlabs), which have a clear aperture of 4mm. Lenses L5 ($f=50\text{mm}$, AC254-50-A, Thorlabs) and L6 ($f=150\text{mm}$, AC254-150-A, Thorlabs) further conjugate the aperture of the galvanometer to the 10.8mm diameter rear pupil of a 10x, NA 0.3 objective O1 (PL FLUOTAR 10/0.3, Leitz). The sample, mounted on a three axis nanopositioning stage (NanoMax301, MELLES GRIOT), was placed in front of the objective. The light that is scattered when going through the sample was collected by another 10x, NA 0.25 objective O2 (PL 10/0.25, Leitz), focused by an imaging lens L7 ($f=200$, AC254-200-A, Thorlabs) and then split into two orthogonal paths with a 10/90 beam splitter SB (BNP26K05510/90, RMI). 90 percent of light was fed into a PMT (H7422-20, Hamamatsu) for fast intensity measurement. A $20\mu\text{m}$ diameter pinhole (PH) was placed in front of the PMT to collect light from a $1.63\mu\text{m}$ diameter area on the object plane. Another 10 percent of the light was captured by a CCD camera (M1400, Dalsa) for monitoring the change of the speckle pattern with a 5ms exposure time. To adjust the power of the laser, a polarizer was mounted on the output port of the laser, which is not shown in the figure.

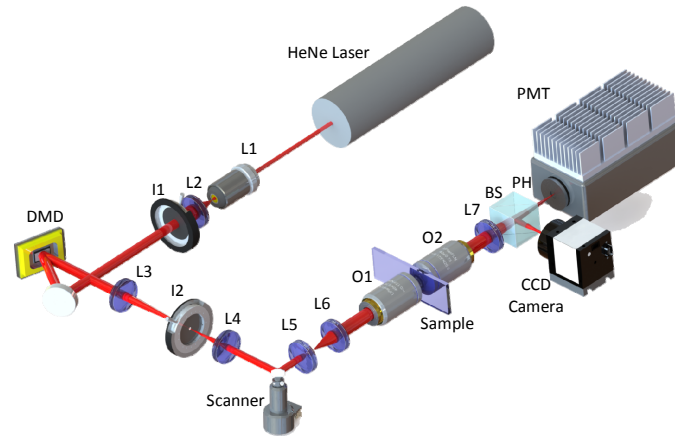


Figure 2. Experimental setup for interferometric focusing by binary measurement of the transmission matrix. The laser output from a HeNe laser (wavefront length $\lambda=633$) is expanded by the lenses L1 and L2 and limited by an iris (I1). The beam covers the whole aperture of the DMD and is relayed by lenses L3 and L4 to a scanner. The unwanted high order beam is blocked by another iris (I2). The beam is further relayed by lenses L5 and L6 and focused on the sample by an objective lens (O1). The diffuse light after the sample is collected by another objective lens (O2) and focused on the PMT and a CCD camera by lens L7. The beam is divided by a 10/90 beam splitter (SB). A pinhole (PH) is installed in front of the PMT to collect the light only from the target.

The intensity modulation process includes the four following steps. The first step is the reference intensity optimization. A galvanometer steers the beam with the target point at the center of the travel when all mirrors are in the full on-state. The second step is the measurement of the binary TM. A sequence of preloaded Hadamard basis images is displayed on the DMD at the full speed of 22.7 kHz. In the third step, the binary TM is calculated and the data on the final mask is transferred to the DMD driver board. In the final step, the new mask is updated on the DLP and the exposure of the camera is triggered. To automate the above process, a customized program running on a personal computer (Dell Precision T3610) was developed in C++. The OpenCV library, optimized for Intel multi-core processors, was utilized to minimize the calculation time. When the 1024 Hadamard modes are applied during measurement and the exposure time of the camera is set as 5ms, the system can operate at 80 ms/frame as shown in Fig. 3(a). Fig. 3(b) shows the time graph for one correction. The first 22ms is spent on the reference intensity optimization. It is followed by an interval of 45 ms for the measurement of the binary TM. Then the calculation and data transfer takes another 8 ms. The total time for one correction before the camera exposure is 75ms. In Section 3, 1024 Hadamard modes are applied.

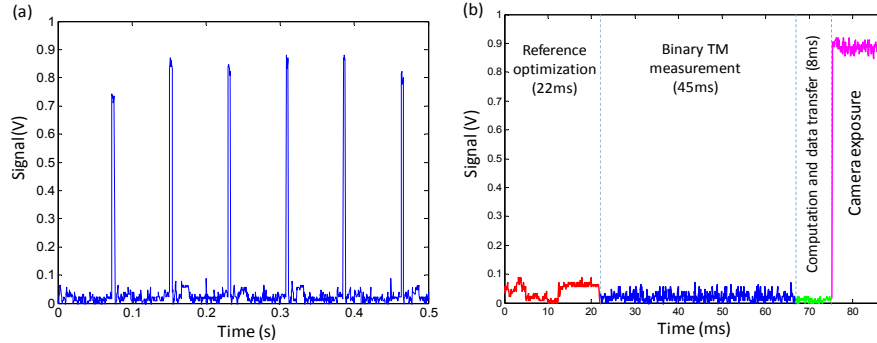


Figure 3. Timing graph of the signal from PMT during system operation (a) and an enlarged time graph for one correction (b).

3. EXPERIMENTAL RESULTS

To focus light through the embryo, two experiments were performed in series. First, dynamic modulation was applied. The mask is refreshed every 80ms. Then images were recorded with an exposure time of 5ms for about 15 seconds. Next, we kept the same configuration but the images were captured with the same mask obtained from the first modulation. The enhancement with both dynamic modulation (blue) and single correction (red) during the first 15 seconds is shown in Fig. 4(a). The enlarged plot during the first 4 seconds is shown in Fig. 4(b). Figures 4(c) and 4(d) show the images at 0.8s, 1.28s, 3.52s and 5.04s for dynamic modulation and single modulation, respectively. The intensity mask is also shown at the lower left corner of each image. After turning on the binary intensity modulation, a sharp focus spot was achieved at the back side of the embryo after the first correction, as shown in the first image from the left in Fig. 4(c). With a single modulation, the static mask cannot compensate the dynamic change of the inner structure of the embryo. At the decorrelation time of 3.5s, the enhancement decays to almost one half as shown in Figs. 4(b) and 4(d). However with dynamic modulation, a stable focus is achieved with the enhancement around 50, as shown in Fig. 4(c). During the operation time of 15 seconds, the system can keep the enhancement at the mean of 50.3 and standard deviation of 6.36. Although the sample has a decorrelation of 3.5 seconds, the fast modulation ability can still benefit the intensity enhancement as shown in the images at 1.28s in Figs. 4(c) and 4(d).

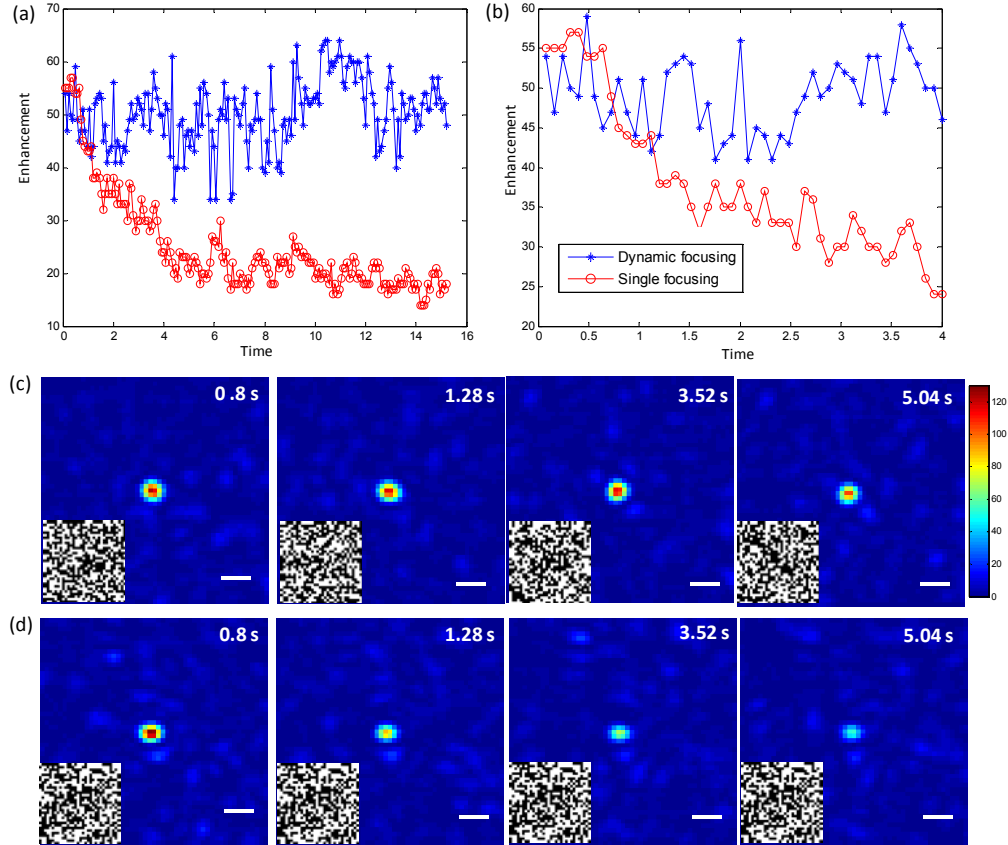


Figure 4. Focusing light through a live drosophila embryo. (a) The enhancement for single and dynamic modulation during the first 15 seconds is shown as the red and blue curves respectively. The enlarged view during the first 4 seconds is shown in (b). The images from the CCD camera at 0.8, 1.28, 3.52 and 5.04 seconds is shown in (c) and (d) with dynamic and single modulations, respectively. The lower left corner of the images shows the corresponding mask on the DMD. Scale bars, $5\mu\text{m}$. (Media 6)

4. Conclusion

We report a high-speed interferometric focusing method to compensate dynamic scattering in live biological tissue based on the fast measurement capability of the binary TM. By using the Hadamard basis, the interference between the optical fields from the reference and each basis element is achieved by displaying the summation of a matrix with all ones and the Hadamard basis elements on the DMD. To overcome the estimation error caused by the low intensity of the reference field at the target, a reference optimization method is demonstrated which can give much more stable focusing during two dimensional scanning. By using a fast DMD as the binary intensity modulator, the proposed method can achieve a 75ms measurement time and an 80ms system refresh time. Although the proposed system is slower than the phase modulation method using an off-axis digital holograph made with a DMD [10, 11], the higher diffraction efficiency of the proposed method would give a higher SNR during interferometric measurement for multi-photon florescence imaging. The experiments with a live drosophila embryo show its advantage for manipulation of light in live biological tissue. The ability to use the intensity from the target for calculation of the binary TM makes it suitable for fluorescence imaging and targeting. As a fast, simple, power-efficient and low-cost solution to deliver light through biological tissue, it has potential for a wide range of applications from basic biological research to clinical investigations.

REFERENCES

- [1] Kubby, J. A. (Ed.), [Adaptive Optics for Biological Imaging], CRC, (2013).
- [2] Popoff, S. M., Lerosey, G., Fink, M., Boccarda, A. C., and Gigan, S., “Controlling light through optical disordered media: transmission matrix approach,” *New J. Phys.* **13**, 123021 (2011).
- [3] Mosk, A. P., Lagendijk, A., Lerosey, G., and Fink, M., “Controlling waves in space and time for imaging and focusing in complex media,” *Nat. Photonics* **6**, 283–292 (2012).
- [4] Popoff, S. M., Lerosey, G., Carminati, R., Fink, M., Boccarda, A. C., and Gigan, S., “Measuring the transmission matrix in optics: an approach to the study and control of light propagation in disordered media,” *Phys. Rev. Lett.* **104**(10), pp. 100601 (2010).
- [5] Popoff, S. M., Lerosey, G., Fink, M., Boccarda, A. C., and Gigan, S., “Image transmission through an opaque material,” *Nat. Commun.* **1**(6), 81 (2010).
- [6] Vellekoop, I. M., Lagendijk, A., and Mosk, A. P., “Exploiting disorder for perfect focusing,” *Nat. Photon.* **4**, 320–322 (2010).
- [7] Vellekoop, I. M. and Mosk, A. P., “Focusing coherent light through opaque strongly scattering media,” *Opt. Lett.* **32**(16), 2309–2311 (2007).
- [8] Katz, O., Small, E., Bromberg, Y., and Silberberg, Y., “Focusing and compression of ultrashort pulses through scattering media,” *Nat. Photon.* **5**, 372–377 (2011).
- [9] Akbulut, D., Huisman, T. J., van Putten, E. G., Vos, W. L., and Mosk, A. P., “Focusing light through random photonic media by binary amplitude modulation,” *Opt. Express* **19**(5), 4017–4029 (2011).
- [10] Conkey, D. B., Caravaca-Aguirre, A. M., and Piestun, R., “High-speed scattering medium characterization with application to focusing light through turbid media,” *Opt. Express* **20**(2), 1733–1740 (2012).
- [11] Caravaca-Aguirre, A. M., Niv, E., Conkey, D. B., Piestun, R., “Real-time resilient focusing through a bending multimode fiber,” *Opt. Express* **21**(10), 12881–12887 (2013).
- [12] Goorden, S. A., Bertolotti, J., and Mosk, A. P., “Superpixel-based spatial amplitude and phase modulation using a digital micromirror device,” *Opt. Express* **22**(15), 17999–18009 (2014).
- [13] Zhang, X., Kner, P., “Binary wavefront optimization using a genetic algorithm,” *Journal of Optics* **16**, 125704 (2014).
- [14] Jang, J., Lim, J., Yu, H., Choi, H., Ha, J., Park, J., Oh, W., Jang, W., Lee, S., and Park, Y., “Complex wavefront shaping for optimal depth-selective focusing in optical coherence tomography,” *Opt. Express* **21**(3), 2890–2902 (2013).
- [15] A. Hedayat, W. D. Wallis, “Hadamard matrices and their applications,” *Annals of Statistics* **6** (6), 1184–1238, (1978).
- [16] Goodman, J. W., [Statistical Properties of Laser Speckle Patterns], Springer-Verlag, Chap. 2, 8–75 (1975).
- [17] Vellekoop, I. M. and Aegerter, C. M., “Focusing light through living tissue,” *Proc. SPIE* 7554, 755430 (2010).